Daily stream temperature predictions for free-flowing streams in the Pacific Northwest, USA

Jared E. Siegel[1,2], Aimee H. Fullerton[3], Alyssa M. FitzGerald[4,5], Damon Holzer[6], and Chris E. Jordan[7]

1: Current affiliation: PACE Engineers, Inc. 3501 Colby Ave Suite 101, Everett, WA 98201, USA. ORCID 0000-0002-9177-4284

2: Former affiliation: Ocean Associates Inc., contracted to Northwest Fisheries Science Center, National Marine Fisheries Service, National Oceanic and Atmospheric Administration, 2725 Montlake Blvd. East, Seattle, WA, 98112, USA

3: Fish Ecology Division, Northwest Fisheries Science Center, National Marine Fisheries Service, National Oceanic and Atmospheric Administration, 2725 Montlake Blvd. East, Seattle, WA, 98112, USA. ORCID 0000-0002-5581-3434

4: Institute of Marine Sciences, University of California Santa Cruz, 1156 High St., Santa Cruz, CA 95064, USA; ORCID 0000-0002-9850-2003

5: Fisheries Ecology Division, Southwest Fisheries Science Center, National Marine Fisheries Service, National Oceanic and Atmospheric Administration, 110 McCallister Way, Santa Cruz, CA 95060, USA

6: Conservation Biology Division, Northwest Fisheries Science Center, National Marine Fisheries Service, National Oceanic and Atmospheric Administration, 2725 Montlake Blvd. East, Seattle, WA, 98112, USA

7: Conservation Biology Division, Northwest Fisheries Science Center, National Marine Fisheries Service, National Oceanic and Atmospheric Administration, 2032 SE OSU Drive, Newport, OR, 97365, USA; ORCID 0000-0002-1557-3624

Corresponding authors: Jared Siegel derajlegeis@gmail.com; Aimee Fullerton aimee.fullerton@noaa.gov

Keywords: statistical model, climate change, snowpack, GAM, stream temperature, hydrology, salmon

Short title: Daily stream temperature predictions for the PNW

Abstract

Supporting sustainable lotic ecosystems and thermal habitats for cold-water species like salmonids requires estimates of stream temperature that are high in scope and resolution across space and time. We combined and enhanced elements of existing stream temperature models to produce a new statistical model to address this need. This model reflects mechanistic processes using publicly available climate and landscape covariates in a Generalized Additive Model (GAM) framework. We allowed covariates to interact while accounting for nonlinear relationships between temporal and spatial covariates to better capture seasonal patterns. Additionally, to represent variation in sensitivity to climate, we used a moving average of antecedent air temperatures over a variable duration linked to area-standardized streamflow. The moving average window size was longer for reaches classified as having a snow-dominated hydrology, especially at higher flows, whereas window size was relatively constant and low for reaches having rain-dominated hydrology. Our model's ability to capture the temporally variable impact of snowmelt on stream sensitivity helped improve its capacity to predict stream temperature across diverse geography for multiple years. We fit the model to stream temperature data from 1993-2013 and used the model to predict daily stream temperatures for ~222,000 free-flowing stream reaches across the Pacific Northwest from 1990-2017. Our daily model fit well (RMSE = 1.76; MAE = 1.32 °C). Spatial and temporal cross-validation suggested that the model produced useful predictions at unsampled locations and across diverse landscapes and climate conditions. We produced stream temperature predictions that will be immediately useful to natural resource practitioners in the Pacific Northwest, USA, especially for effective conservation planning in lotic ecosystems and for managing species such as Pacific salmon. Our approach is straightforward and can be easily adapted to new spatial regions, time periods, or scenarios such as anticipated changing snowmelt patterns with climate change.

Introduction

The critical role water temperature plays in governing aquatic biological processes and reflecting fluvial system health and function drives our desire to understand riverine thermal regimes and has motivated the development of stream temperature models for decades [1]. In recent years the rate of model development has increased substantially [2]. While water temperatures are increasing and expected to continue to increase across the globe with climate change, empirical observations remain relatively sparse, making stream temperature modeling a pressing need for the water resources community [3,4]. However, riverine thermal regimes will change at different rates in different places, as governed by local climate and landscape characteristics [5]. Having accurate predictions of water temperature over space and time under diverse climate conditions will be important to inform conservation practitioners' work, especially for cold-water aquatic species such as salmonids. Because many cold-water species are already living near their maximum thermal tolerances, they are likely to be particularly challenged by changing thermal regimes and thus reflect pressing land and riverscape management needs [6:10].

Climate interacts with landscape spatial heterogeneity, stream flow rates, and stream network connectivity to produce complex spatiotemporal patterns in stream temperature. This makes stream temperature prediction a multi-faceted, dynamic, space-time problem [11,12]. Different modeling approaches have been developed to address this need, ranging from practical models that are not overly complex (e.g., regression models) to complex models that are more difficult to apply yet better represent complex physical processes (e.g., process-based models or models that merge process-based and statistical methods). Complex process-based stream temperature models often track thermal energy budgets through a riverscape over time and aim to reflect mechanistic links between environmental variables and water temperature [13,14]. However, they tend to be data-hungry, time-consuming to develop and run, and are typically applied over limited spatial extents such as the Sacramento River [15].

In contrast, regressions and other statistical models typically rely on fewer data, simpler relationships, and require less expertise to develop and run [16:18]. These models can, however, suffer from spatial autocorrelation problems that occur when trying to predict stream temperature across a directed-flow connected network, stemming from the underlying processes of water and energy flow [11,19]. Spatial statistical network (SSN) models were developed to address this concern. They use autocovariance functions that are assumed to be stationary across the spatial domain over which models are fit [12,20]. To date, SSN models applications have generally limited predictions to coarse

temporal resolution like seasonal or monthly means [5,21] or to small spatial extents [12,22]. Because SSN models depend on substantial data to inform their spatial autocovariance functions, they are limited in their ability to predict outside the spatial or temporal bounds of the data used to fit the model. Therefore, SSN models may not predict well in scenarios where the correlation structures are poorly informed or likely to shift, e.g., with landscape alteration or climate change. There is, therefore, a strong, immediate need to enhance statistical models to better predict stream temperature under dynamic climate conditions.

Statistical models can capture dynamic and changing conditions if parameterized covariate relationships are able to adequately represent seasonally shifting and interacting processes that influence stream temperature [23]. Numerous studies have compared the performance of model types against each other, offering varying conclusions regarding the best modeling approach [13,24:26]. However, model performance has as much to do with the ability of covariates to capture variation in drivers as it does with the model type and statistical methods. We argue that there is substantial room for improvement by carefully choosing and parameterizing covariates to better reflect underlying processes driving energy fluxes.

Previous statistical stream temperature models have generally assumed non-interacting climate (e.g., air temperature, precipitation) and landscape covariates (e.g., elevation, drainage area, slope) [11,21,27,28]. In a recent advancement, Siegel and Volk [23] allowed time-varying climate covariates (e.g., air temperature) and spatially-explicit landscape covariates (e.g., elevation) to interact, thereby producing a model that predicted stream temperatures based on putative mechanistic principles (defined *a priori*), rather than allowing a covariance function to absorb error that was otherwise unexplained. They argued that these interactions were necessary for models to fit across seasonal and interannual climate variability as the influence of many variables is not unidirectional. Instead, most spatial variables either mitigate or amplify seasonal extremes in stream temperatures, and thus the directional influence of variables changes between cold and warm seasons. For example, groundwater influence can mitigate temperature extremes, cooling river water in the summer but warming it in the winter. Spatiotemporal thermal variability across the entire year was well approximated by these simple interaction terms between spatial landscape covariates and temporal climatic covariates [23,29,30].

Many statistical models use air temperature as a proxy to represent physical energy exchanges driven by solar radiation and thermal conduction (e.g., [31]). However, as with the example of groundwater above, the relationship between air temperature and stream temperature can change across seasons and years as it is mediated by snowmelt and river discharge [24,32,33]. For example,

snow-influenced streams may be less sensitive to air temperatures due to the direct cooling influence of snowpack melt and associated higher flows creating increased thermal inertia [34]. Stream temperature becomes more correlated with air temperature in low snowpack years and later in the season as the snowpack diminishes and associated flows decline.

Siegel et al. [35] represented temporal variation in the sensitivity of stream temperature to air temperature by developing a covariate of antecedent air temperature averaged over a variable duration that was determined by flow conditions. They used this covariate (and others) to estimate stream temperatures at ~400 free-flowing sites (i.e., uninfluenced by impoundment) throughout the Pacific Northwest (PNW), USA. They found evidence that snowpack buffered stream temperature long after snow had melted, presumably due to its movement into subsurface waters that later emerged into streams via the hyporheic aquifer. Thus, sites with higher snowpack had longer thermal lags than sites uninfluenced by snow, making the snow-influenced sites less responsive to short-term changes in air temperature. Asarian et al. [36] used a similar approach that included time-varying and nonlinear effects of flow to predict stream temperature for a snowmelt-driven watershed in California. They also found that stream temperatures remained lower well into summer in high flow years. Both studies fit models to single sites, thus their approach did not capture interactions between climatic and landscape influences on stream temperature.

Here, we improve on previous approaches by incorporating the antecedent air temperature covariate introduced by [35] (referred therein as “flow-dependent flexible-lag air temperature”) into the spatiotemporal modeling approach of [23] using publicly available spatially and temporally continuous climate covariates in conjunction with spatially continuous landscape covariates. We present a daily stream temperature model applicable across the entire year for the geographically diverse PNW, a region critical for cold-water salmonid production. We fit the model to stream temperature data from 1993-2013 and used the model to predict daily stream temperatures for all regional stream reaches from 1990-2017. Our results illustrate spatial and temporal variation in stream temperature that can be used directly in management applications now and that may also generate insights about how stream temperatures will be affected by climate change.

Methods

Study region and spatial network

For our spatial framework we used the National Hydrography Dataset 1:100k (NHDPlus version 2) network of stream reaches created by the US Geological Survey [37]. The PNW portion of the dataset (Region 17) is primarily composed of Columbia River Basin streams in the USA, but also includes coastal areas of Oregon and Washington and Puget Sound drainages. It includes >232,000 stream reaches of 1.98 km in length on average (SD = 1.74 km), >94% of which were free-flowing. As in [35], we classified free-flowing streams as those upstream of the influence of major dams, i.e., those with capacity >0.1 km^3 from the Global Reservoir and Dam Database (GRanD v1.3; [38]) and those with height >15.24 m (50 ft) from the National Inventory of Dams (https://nid.usace.army.mil). In contrast to [35], we also included streams with minimal dam influence in our definition of free-flowing reaches. To calculate dam influence, we calculated the percentage of the upstream drainage area (PDA) for each reach that lies upstream of a major dam. For fitting models, we implemented a conservative cutoff, only including reaches where PDA < 5%. We used the resulting model to predict stream temperatures for reaches with a PDA up to 25%. When more than 25% of the flow in a reach comes through a large dam, the temperature in that reach is frequently uncoupled from the physical processes we modeled (e.g., when water is released from below the thermocline in deep reservoirs, or when warm surface water is spilled over dams at unnatural times). The free-flowing streams in our dataset comprised small to large streams (stream order mean 1.8, max 9), represented a large range of elevations (mean 1200 m, range 0-3362 m), and included headwater streams with minimal drainage areas to large rivers with drainage areas > 600,000 km^2.

Stream temperature

We used ~20 years of daily stream temperatures from 1993 through 2011-2013 (with the end year varying by region) that were contributed by various organizations to the NorWeST project; raw data were curated, quality controlled, summarized, and made publicly available by the USDA Forest Service [5]. We downloaded “All Days Daily Summary” files within the PNW study region, which included individual stream temperature measurements typically taken at 15-30 min intervals that had been summarized into daily metrics (https://www.fs.fed.us/rm/boise/AWAE/projects/NorWeST/StreamTemperatureDataSummaries.shtml).

We used ~5.0 million daily stream temperature estimates for free-flowing reaches (88% of ~5.7 million available, after excluding data from reaches heavily influenced by dams) (Fig 1).

Fig 1: Locations of daily stream temperature data from NorWeST that we used to fit our model, filtered to omit any locations influenced by large dams.

Antecedent air temperature covariate

To reflect variation in the sensitivity of stream temperature to changes in air temperature, we used a covariate of air temperature averaged over an antecedent period, the length of which varied in conjunction with flow conditions. The rationale for including this covariate was to account for temporal variation in thermal inertia caused by dynamic processes that alter the rate at which streams warm (e.g., precipitation stored as snow and subsequent snowmelt-driven increases in flow) and processes that add direct inputs of cooler water that suppress stream temperatures in comparison to air temperatures (e.g., groundwater and snowmelt). Our antecedent air temperature covariate (*Tl*) was adapted from the approach described in [35], as outlined below.

Siegel et al. [35] found that water temperature in snowpack-influenced streams demonstrated slower responses to changes in air temperature than rain-dominated streams, even after the snowpack had melted. Specifically, they described that the average window size over which antecedent air temperature was most highly correlated with stream temperature tended to be larger in snowpack-fed streams. Based on their results, we categorized each stream reach by the average snow-water-equivalent (SWE) accumulated within its drainage area (*Sws*) for each year and defined each reach and year combination as having “rain-dominated” (<20 mm), “transitional” (20-100 mm), or “snow-dominated” (>100 mm) hydrology. The average SWE was calculated by averaging all daily values across the year, including days with no snowpack, and thus the metric reflects the duration of snowpack as well as the magnitude of accumulation. In contrast to [35], we used annual SWE accumulation rather than the multi-year average, which allowed each reach to transition between classes among years to better capture interannual variability. These classifications were used only to develop the antecedent air temperature covariate *Tl*; data were not subset by these classes when fitting the stream temperature model.

Next, we developed a metric representing the best moving average window size for each reach and day. To do this, we calculated daily log-scale area-standardized flows (*Qr*) by subtracting estimated average annual flows based on a reach’s watershed area (*A*) from estimated daily mean log-scale flows

from the National Water Model (see below) using the relationship developed by [35]: Qr = -4.10 + 0.93*A. We then split each of the snow-dominated, transitional, and rain-dominated data subsets into 200 groups separated by 0.5% quantiles of Qr. We correlated stream temperature in each Qr quantile with local air temperature averaged over antecedent moving windows of different sizes (1, 3, 6, 9, 12, 15, 20, 25, 30, 40, 50, and 60 days including the day of prediction). To identify the optimal window size (number of days) over which air temperature would be averaged for each hydrographic classification, we fit Generalized Additive Model (GAMS, [39]) smoothers with <6 knots using the R package mgcv [40] for rain, transitional, and snow data independently, where the response variable was the window size with the highest correlation from the previous step, and the explanatory variable was mean Qr in each quantile. Finally, we rounded the predicted window size to the nearest tested window size and created the antecedent air temperature covariate (Tl) by selecting the air temperature associated with the optimal window size for each daily value of Qr.

Other covariates

We selected commonly used model covariates that represent well-known drivers of stream temperature; see [41] for a summary of energy flux processes. Our sources for climate data were: daily mean air temperatures from the PRISM Climate Group at Oregon State University ([42], http://prism.oregonstate.edu); daily modeled snowpack data represented as snow water equivalent (SWE) provided by the National Snow and Ice Data Center [43]; and daily flow predicted by the National Water Model Version 2 [44]. The air temperature data and SWE data are available as continuous 4-km (16-km^2) grid cells whereas the NWM flow predictions are available for each reach in the NHDPlus version 2 stream network. To produce distinct local- and watershed-scale air temperature and snowpack covariates, we averaged gridded data over the local area draining directly into a NHDPlus version 2 stream reach and over the entire upstream area draining to a reach. For our local air temperature covariate, we used the antecedent air temperature covariate described above. We also used daylight hours (h) which vary across the year, and reach latitude which defines solar angle irrespective of day length. We included a set of spatial covariates that were temporally static to account for landscape characteristics that may affect stream temperature. Data sources included EPA StreamCat [45] and NHD V2.1 network attributes [37]. In addition, we summarized percent canopy cover along reach streamlines from the National Land Cover Dataset (NLCD). See Table 1 for a full list and description of covariates.

We evaluated the correlation between covariates across seasons (Supp Fig S1). Only two pairs of covariates were highly correlated: Tws and Tl during fall (0.9) and winter (0.8), and $SA1$ and Sws during

winter (0.9). *SA1* and *Sws* were not significantly correlated during the other seasons, so we included both covariates. Although correlated, *Tws* and *Tl* were both included in the model due to distinct hypothesized impacts on stream temperature. An interaction term to help the model distinguish the individual impacts was included and found to be important in informing the model. However, because there is seasonal collinearity between some of the variables, the modeled relationships for these variables predicted by the model should be interpreted cautiously. Still, predictive power was improved by including all variables, and thus some remaining collinearity was considered acceptable as the primary goal of the effort was to produce accurate predictions across time and space.

Table 1: Covariates used in the stream temperature model.

Symbol	Description	Dimensions	Unit	Source
Tl	Antecedent air temperature (summarized by the local reach-contributing drainage area)	daily*reach	°C	This study
Tws	Mean daily air temperature in upstream watershed	daily*reach	°C	PRISM
Sws	Mean daily snowpack snow-water-equivalent (SWE) in upstream watershed	daily*reach	mm	National Snow and Ice Data Center
DL	Day length	daily*reach	hours	
D	Day of year	daily	Julian	
Qr	Mean area-standardized flow	daily*reach	log(m^3/s)	This study
Lat	Reach latitude	reach	Latitude	ArcGIS
E	Mean reach elevation	reach	m	NHDv2.1 attributes
Ed	Difference between the reach elevation and the mean watershed elevation	reach	m	NHDv2.1 attributes
A	Watershed area	reach	log(km^2)	NHDv2.1 attributes
BFI	Percentage of mean flow that comes from base flow	reach	%	NHDv2.1 attributes
S	Slope	reach	gradient proportion	NHDv2.1 attributes
W	Percent of watershed covered in open water	reach	%	StreamCat
I	Percent of watershed covered in ice	reach	%	StreamCat
F	Percent of 100-m riparian buffer that is forested	reach	%	StreamCat
C	Percent canopy cover over reach streamline	reach	%	NLCD
U	Percent of watershed covered in urban land use	reach	%	StreamCat
V	Percent of watershed covered by extrusive volcanic rock	reach	%	StreamCat
P	Mean annual reach-contributing-area precipitation	reach	mm	StreamCat
R	Mean annual reach-contributing-area air temperature range	reach	°C	StreamCat
SA1	April 1st watershed snow-water-equivalent	annual/reach	mm	National Snow and Ice Data Center

Modeling methods

We parameterized the effects of climate covariates using a combination of GAM tensor product smoothers and interactions fit with the "*ti*" function in the R package *mgcv* [40]. Although the default *ti* fitting function using thin-plate regression splines has a penalty term to prevent overfitting, our examination of fitted relationships and cross-validated predictions found it to be too permissive for our purposes. To avoid overfitting and has been done previously, we therefore restricted the number of knots within the climate variable smoothers to limit the complexity of fitted relationships while allowing enough flexibility to capture nonlinear relationships based on theory [23,28]. Because we assumed that the landscape covariates would have primarily linear effects, either amplifying or muting the impact of climate across space, smoothers were not needed. Limiting the number of smoothers simplified the model and lowered the risk of overfitting.

Our modeling approach centered around our primary air temperature covariate (antecedent air temperature *Tl*), which we allowed to have 6 knots to capture the logistic-shaped relationship with stream temperature [31]. Most of the other variables were allowed to interact with *Tl* to parameterize their theoretical impact of either mitigating or exacerbating climate impacts on stream temperature. However, daily watershed averaged air temperature (*Tws*), which was allowed 3 knots, helped account for the large influence of air temperature on a given day. *Tws* was considered a better choice than *Tl* to interact with snowpack (*Sws*) as it better represented air temperatures encountered by mountain snowpack. For other temporally continuous climate covariates (i.e., snowpack *Sws*, area-standardized flows *Qr*, and daylight hours *DL*), we allowed 4-6 knots and included interactions with antecedent air temperature (*Tl*).

Spatial landscape covariates that had no temporal component were modeled with linear effects, as they were expected to have simpler relationships with stream temperature. We allowed each of these variables to interact with antecedent air temperature (*Tl*) to help account for seasonal variation in their influence on stream temperature. For example, covariates that cool stream temperature in the summer when air temperatures are warm, such as groundwater influence (as represented by baseflow index, *BFI*) or riparian forest cover (*F*), tend to warm stream temperature during the winter when air temperatures are cold. We considered only two other interactions between linear covariates: annual April 1st snowpack depth (*SA1*) and day of year (*D*) to help account for the delayed effect of snow melt through groundwater connectivity; and stream elevation (*E*) and watershed area (*A*) to help distinguish high- from low-elevation headwater streams. The final model formula was:

$$T_w = \text{ti}(Tl) + \text{ti}(Tws) + \text{ti}(DL) + \text{ti}(Qr) + \text{ti}(Sws) + \text{ti}(Tws, Tl) + \text{ti}(DL, Tl) + \text{ti}(Qr, Tl) + \text{ti}(Sws, Tws) + Tl*(Lat + E + A + BFI + Ed + S + W + I + F + C + U + V + P + R) + SA1*D + E*A.$$

Validation

To assess the ability of our methods to produce accurate predictions at high spatiotemporal resolutions, we compared the accuracy and precision of predictions from a single model (i.e., a model fit to all available data) and models fit to seasonal and spatial subsets of the data. Prior investigations demonstrated that prediction accuracy improved if models were fit to the warming and cooling seasons separately [23,27]. We therefore split the dataset by the day of year that represented the average peak in stream temperatures in our study (Julian day 210, ~July 29th). For regional models we split the dataset into 8 large sub-regional watersheds within the PNW based on the "processing units" designated in the NorWeST dataset [5]. We then examined the effect of season/region specific models for a total of 16 separate fits.

We validated models using root mean squared error (RMSE) and mean absolute error (MAE) statistics. In addition to providing fit statistics, we performed a leave-one-year-out cross-validation and a leave-one-region-out cross-validation, hereafter referred to as the temporal and spatial cross-validations, respectively. Although cross-validation methods often leave out a random proportion of the dataset, our temporal and spatial cross-validation tests evaluated the model's ability to predict entirely distinct years and regions left out when fitting the model. For the temporal cross-validation, a single year was withheld from the model fitting dataset and used as a validation dataset, whereas for the spatial cross-validation, a region was withheld. The validation processes were repeated until each year/region had been withheld and predicted. For cross-validations, we report root mean squared prediction error (RMSPE) and mean absolute prediction error (MAPE).

Finally, we evaluated if characteristics of data used to fit models (i.e., reaches and days with empirical data) were spatially and temporally representative of those across the entire PNW where we made predictions. Because of the large number of covariates used in our model, for this dataset evaluation we compressed the multidimensional covariate space of both fitting and prediction data using principal components analysis (PCA) and evaluated spatial and temporal covariates separately. All covariates were standardized by relative rank. We compared the spatial covariate space for all reaches in the fitting dataset (n = 8,755) to that of the entire PNW region we predicted (n = 228,538). For the immense temporal dataset (i.e., daily data at each reach), we analyzed a random 10% subset of reaches

and aggregated data by month, resulting in 333,150 unique observations of reach/month combinations. Multiple random subsets were tested and gave similar results to those presented here.

Results

Reach hydrology classifications

Winter air temperature (Fig 2A) and annual precipitation (Fig 2B) both influenced average snowpack accumulation (Fig 2C). Each reach in the PNW was classified as rain-dominated (hereafter, "rain reaches"), snow-dominated (hereafter, "snow reaches"), or intermediate (hereafter, "transitional reaches") based on the mean annual SWE (Fig 2D). We used these hydrology classifications to develop our antecedent air temperature metric *Tl* from an average of 499 rain reaches (mean across years; maximum 1,150), 519 snow reaches (maximum 960), and 518 transitional reaches (maximum 1,053). Note that this subset of reaches used to inform *Tl* were those for which we had empirical stream temperature data (i.e., 8,755 of >232,000 stream reaches). Rain reaches occurred at lower elevations and had warmer air temperatures and lower flows but higher precipitation on average compared to snow reaches (Fig 3). Mean annual watershed snow depths were usually < 500 mm for snow reaches (median = 209 mm, but >2000 mm for some reaches). Environmental characteristics of transitional reaches were generally intermediate to snow and rain reaches, but were more like snow reaches for air temperatures (*Tws*), elevation (*E*), and base flow (*BFI*). However, transitional reaches were drier on average (median annual precipitation of 660 mm, compared to 944 mm and 1176 mm for snow and rain reaches, respectively), suggesting that precipitation represented the primary reason for lower snowpack accumulations in comparison to snow reaches on average.

Fig 2: Maps of the PNW illustrating (A) winter average air temperature and (B) mean annual precipitation from the PRISM dataset, (C) mean accumulated snow water equivalent (SWE) in upstream watersheds from the National Snow Water and Ice Dataset, and (D) regions classified in this paper as having rain-dominated, transitional, and snow-dominated hydrology. The mean accumulated snow water equivalent (SWE) was used to classify the hydrograph classes shown in (D). Here, we show the average snowpack accumulation and most common hydrograph classification across the entire dataset. For the analyses annual values were used.

Fig 3: Environmental characteristics of data designated as having "rain", "transitional", or "snow" dominated hydrographs. Boxplots show medians, interquartile ranges, and ranges across reach/year combinations. Abbreviations: BFI = baseflow index; CMS = cubic meters per second; SWE = snow water equivalent.

Antecedent air temperature

Across hydrology classes (snow, rain, and transitional), the moving average window size used to calculate the antecedent air temperature covariate *Tl* reflected seasonal flow patterns, with the lowest flows occurring during summer and late fall (Fig 4A). Snow reaches demonstrated a strong distinct flow peak during spring snowmelt, whereas rain reaches had elevated flows throughout the late fall and winter that more closely mirrored regional precipitation patterns. The transitional class demonstrated annual flow patterns similar to the snow class, but with an earlier and more modest spring-melt peak.

Moving average window sizes increased with positive *Qr* for snow and transitional data (Fig 4B), but snow data had larger window sizes of around 9 to 12 days at intermediate conditions *Qr* (-1.5 to 0). In contrast, rain data demonstrated relatively smaller window sizes of around 3 to 6 days at all flows. The highest maximum correlations between stream temperature and antecedent air temperature occurred for snow data at mid to low *Qr* (Fig 4C). Maximum correlations were generally lowest for rain data and intermediate for transitional data.

Fig 4: Smoothed patterns for rain, transitional, and snow reaches illustrating (A) area-standardized flow residual (*Qr)* over the year, (B) antecedent air temperature window size with the highest correlation with stream temperature versus average *Qr*, and (C) maximum correlation between stream temperature and antecedent air temperature versus *Qr*.

Stream temperature model performance

We predicted daily stream temperature over 25 years for all stream reaches throughout the PNW in a single model with reasonable accuracy and precision (MAE = 1.30, RMSE = 1.74, Table 2). The combined predictions from models fit to seasonal, regional, and seasonal/regional subsets of the data fit slightly better than the single model (RMSE = 1.68 (-0.04%), 1.62 (-0.07%), and 1.58 (-0.10%) respectively).

Prediction error in the temporal cross-validation procedure (MAPE = 1.31 (+0.01%), RMSPE = 1.75 (+0.01%)) was nearly identical to the single model, demonstrating the ability of the model to expand outside of the temporal parameter space used to fit the model. Prediction error increased slightly more in the spatial cross-validation test (MAPE = 1.44 (+0.11%), RMSPE = 1.88 (+0.08%)), suggesting that model has comparatively more difficulty extrapolating into new watersheds, but that spatial extrapolations may still be useful in many cases.

The available stream temperature data used to fit models were broadly representative of the physical characteristics (Fig 5A) and of the temporal variation of climate covariates during the study period (Fig 5B) across the Pacific Northwest region where we made predictions of stream temperature. For the spatial PCA, three axes were significant and explained 66.3% of the total variance. The spatial covariates with the highest loadings were canopy cover (C), precipitation (*P*), forested riparian buffer percentage (*F*), and annual temperature range (*R*) (Table S1). PC1 (28.8% of variance) predominantly explained variation associated with forest cover and regional climate characteristics; PC2 (21.9 %) was associated with geomorphology, and PC3 (15.6%) included elevation and similar elements as the first two axes. For the temporal PCA, three axes were significant and explained 83.1% of the total variance. The temporal covariates with the highest loadings were watershed temperature (*Tws*), antecedent air temperature (*Tl*), and day length (*Dl*) (Table S2). PC1 (35.3%) predominantly explained variation associated with air temperature, PC2 (29.7%) was associated with streamflow, and PC3 (18.0%) centered on the snowpack.

Table 2: Statistics of model fit (°C) and temporal (tXV) and spatial (sXV) cross-validation predictions for a single model fit to the entire dataset and for models fit to regional, seasonal, or seasonal/regional subsets of the data (n = number of models). Statistics are shown for daily predictions and for monthly averages (note: not all month/site combinations had data for the entire month and in these cases the available data were averaged for the month). RMSE = root mean squared error; MAE = mean absolute error; RMSPE = root mean squared prediction error; MAPE = mean absolute prediction error.

	Single	Seasonal (n = 2)	Regional (n = 8)	Seasonal/regional (n = 16)
RMSE	1.74	1.68	1.62	1.56
MAE	1.30	1.25	1.20	1.15
RMSE_Month	1.55	1.50	1.43	1.38
MAE_Month	1.14	1.10	1.04	0.99
RMSPE_ tXV	1.75	1.69	1.65	1.60
MAPE_ tXV	1.31	1.26	1.22	1.18
RMSPE_Month_ tXV	1.56	1.51	1.45	1.42
MAPE_Month_ tXV	1.15	1.11	1.06	1.02
	1.88	1.83	NA	NA

RMSPE_ sXV				
MAPE_ sXV	1.44	1.40	NA	NA
RMSPE_Month_ sXV	1.69	1.65	NA	NA
MAPE_Month_ sXV	1.28	1.24	NA	NA

Fig 5: PCA of (A) spatial and (B) temporal covariates used in the stream temperature model, indicating that reaches and days with empirical data that were used when fitting models (magenta) are broadly representative of the parameter space for predicting into locations throughout the full region (gray). The spatial dataset used all data; the temporal dataset used a random 10% of reach-days, aggregated by month.

Covariate effects on stream temperature

As intended when designing our model, much of the variation in stream temperature predictions was associated with air temperature metrics: the antecedent air temperature at a local reach (*Tl*) and the mean daily air temperature in the upstream watershed (*Tws*). Both *Tl* and *Tws* had roughly equal impacts on stream temperature as shown through their interaction with each other (Fig 6A). In addition, interactions between air temperature covariates and other covariates allowed a shift in directional impact in accordance with theory (e.g., *BFI* and *Ed* and *A*). Daylength (*DL)* was important at higher values, consistent with the expectation that air temperature is more related to stream temperature drivers when days are longer (Fig 6B). Area-standardized flows (*Qr*) were also important at higher values, which likely reflects effects of snowmelt that was not fully captured in *Tl* (Fig 6C). Higher values of daily snowpack in the upstream watershed (*Sws*) led to lower stream temperature predictions when air temperatures in the upstream watershed (*Tws*) were above 0 °C, reflecting the direct cooling influence of snowmelt (Fig 6D). We note that the influence of snowmelt on higher flows is also captured indirectly in *Qr* and *Tl*. In addition to the daily snowpack metric (*Sws*), annual April 1st snowpack (*SA1*) had a slightly negative relationship with stream temperature (~ 1 °C per 1m), which was stronger after the snowpack had melted (Supp Fig S1).

Some of the more influential spatial covariates lacking a temporal component included reach elevation (*E*), the difference between the reach elevation and the average watershed elevation (*Ed*), watershed area (*A*), a representation of base flow (*BFI*), and the percent riparian forest cover in the 100-m buffer (*R*) (Fig 6E-H). The relationship between *Tl* and *E* suggests that streams at higher elevations are generally cooler irrespective of air temperature, which is already accounted for in the model (Fig 6E),

whereas *Ed* suggests that at high air temperatures, streams that drain steeper and higher elevation basins are generally cooler (Fig 6F). The relationship between *Tl* and *A* suggests that headwater streams are less sensitive to air temperature, which may reflect greater relative groundwater or snow influence (Fig 6G). Similarly, streams with high *BFI* (the covariate best representing potential influence of and connection to subsurface flow pathways) are also less sensitive to air temperatures (Fig 6H). Finally, streams with higher riparian forest cover (*R*) tended to be cooler at higher air temperatures, representing shading from solar radiation during growing seasons when trees have foliage (Fig 6I). For completeness, we provide additional conditional effects plots for temporal and spatial covariates in Supp Figs S2-4.

Fig 6: Conditional effect plots for climate and landscape covariates. All interactions we included in the model are shown. Contours represent 1 °C variation in predicted stream temperature. White dots represent empirical data. See Table 1 for covariate definitions.

Discussion

In this work, we present a novel stream temperature modeling framework that extends previous efforts [5,21,23,35,36]. We applied our model to predict stream temperature at fine temporal (i.e., daily) and spatial (i.e., reach) resolutions across the broad spatial extent of the PNW (Fig 7). Using publicly available data and a straightforward statistical GAM framework, we provide daily predictions for 222,321 free-flowing stream reaches from 1990 through 2017. Our model performed well outside the spatial and temporal extent of the data used to inform the model, suggesting that our model captured many of the complex and interacting drivers that determine stream temperature. These results should be immediately useful in conservation planning for lotic systems of the PNW that support cold-water species such as salmonids. Our approach is straightforward and can be easily adapted to new spatial regions or time periods.

Fig 7. Stream temperature predictions averaged by season (top panel: summer; bottom panels: spring, fall, winter) to illustrate of the spatial extent over which predictions were made and temporal variability. Values were mapped to individual reach-contributing areas to improve visualization, but daily data are linked to each stream reach identifier in the National Hydrography Dataset version 2. Gray indicates reaches where we did not make predictions such as in reservoirs or because reaches were heavily influenced by dams (PDA > 0.25).

Model utility

The performance of our model compared favorably to other statistical stream temperature models recently applied in the western USA [5,21,23] that produced prediction errors of around 0.5 to 2 °C. However, our objectives were more ambitious than most other models in that we predicted daily rather than coarser metrics such as mean monthly stream temperature [5,21], across a broad geographic region rather than within individual watersheds [23], and across the entire year in contrast to seasonally [46]. Although our results demonstrated that predictions were improved by fitting models to smaller spatial or temporal extents, average prediction errors were only 0.1 to 0.2 °C better than the single model, an improvement that is small enough to be within the error range of most measuring devices.

The flexibility of our statistical model structure was essential to its ability to accurately predict across a geographically diverse region characterized by substantial seasonal and interannual climate variability. Most previous models did not explicitly account for hydrograph class (snow, rain, or transitional) despite that previous research has clearly demonstrated that the amount of winter precipitation falling as snow can strongly influence stream temperature and its relationship with air temperature across multiple seasons [24,32,35,47]. Also, previous statistical models typically used linear, non-interacting effects of air temperature on stream temperature, which does not reflect the nonlinear and spatiotemporally variable nature of this relationship [48,49 but see 36]. Our model overcame these limitations by including (1) an antecedent air temperature metric that was dependent on snowpack and flow, (2) nonlinear relationships, and (3) covariate interactions primarily with air temperature that allowed the influence of covariates to shift seasonally as theoretically expected. For example, streams with high base flow (BFI, which represents groundwater influence) should be (and were) less sensitive to air temperature, and therefore should be (and were) warmer in the winter and cooler in the summer on average compared to streams with low base flow. These adaptations allowed us to better capture the dynamism of the air-stream temperature relationship and overcome a known drawback of linear statistical models [13,14].

A common concern in using GAMs is that relationships can be over-fit, capturing small patterns in the data that are not caused by covariate influences [39]. Following previous research, we limited model complexity by reducing the number of smoother knots [23,28]. Automated parameter penalties within the fitting functions of the modeling package alone led to overfit relationships. The success of our model in the cross-validation tests suggests that our model is not over-fit, and other research has supported GAMs as appropriate statistical models for stream temperature [25,26,28]. In addition, the

relationships parameterized in our statistical model align with theoretical expectations, as demonstrated in conditional effects plots (Figs 6 and Supp Figs S2-4). These results support our decisions to limit model complexity by constraining the number of knots in climate variable smoothers and to fit linear relationships to temporally constant variables. Visually examining concordance between expected and observed conditional effects is an important model quality control step when considering covariates to include in a model [13,23].

Our statistical model was less expensive in data requirements, expertise, execution time, and computing power than a more complex process-based model. The diversity of spatial and temporal scales and physical forcing pathways that drive stream temperature over broad spatial and temporal extents is so vast as to make purely mechanistic physical models impractical [13,14,16:18]. The variables we used in this model are publicly available throughout the contiguous United States, although retrospective expansion is limited by the historical availability of the climate metrics. Our results suggest that statistical methods that can generally and robustly model patterns that emerge from physical processes are an appropriate compromise between physical process representation and data and computational requirements.

Our model successfully predicted stream temperatures outside of the spatiotemporal bounds of the data used to fit the model, suggesting that our model's statistical relationships represented mechanistic controls and can therefore be useful in predicting stream temperatures under un-monitored conditions. Some statistical models have shown poor prediction accuracy when extrapolating to novel time periods or regions (e.g., [48,50]). This likely stems from a combination of extrapolating predictions to streams with dissimilar hydrological classes and not including variables that represent distinct thermal regimes. The ability of our model to extrapolate predictions was improved by fitting the model across a large, geographically diverse region and over multiple decades representing substantial interannual climate variability. Accordingly, data in temporal expansions (e.g., filling gaps or extending time-series) or spatial expansions (e.g. predicting in adjacent basins) are more likely to be represented in the wide-ranging covariate space used to inform the model and thus more accurately predicted.

Potential applications

Our model's ability to predict temperature across a large range of spatiotemporal scales makes it a powerful tool for informing and supporting species and habitat management. Predictions can be used for evaluating different management and restoration scenarios [51,52]. For example, consulting maps of predicted stream temperature during times of potential ecological stress may indicate where

increased riparian shade, floodplain reconnection, or other temperature-moderating actions might be necessary to improve ecosystem function. If our modeling framework were to be applied in other regions, a cross-region comparison could provide information useful for considering whether management approaches that have worked well in one region may be applicable in another.

For protected cold-water species like salmonids, a potential application of our results could be to evaluate thermal habitat across life history stages to guide management strategies. Our stream temperature predictions can help determine if management actions should resist change (e.g., conserve functional thermal habitat), accept change (e.g., recognize that some habitats are unlikely to become as functional as they may have been in the past), or direct change (e.g., actively alter stream temperatures or move sensitive species) [10]. For example, our predictions can identify streams that are more stable throughout the year, such as snowpack-influenced or groundwater-fed streams. Streams with stable thermal regimes can be more productive than regulated reaches, and may be more resistant to climate change, making them better targets for species re-introductions [24,53:56]. As another example, our model could help practitioners envision potential stream temperatures as if a dam did not exist (since we did not model dam effects), which may be useful for assessing dam management and/or removal strategies.

Another powerful application of our model would be to predict the effects of climate change on stream temperature. The model successfully predicted stream temperature outside of the spatiotemporal bounds of the data used to fit the model, so it is likely to perform well in unsampled time periods. Our methods provide improvements for parameterizing the seasonal and annual impacts of snowpack and associated flows, which are expected to be strongly influenced by climate change. In addition, fitting the model across such a large and diverse region across numerous climatically distinct years will likely be beneficial in predicting climate impacts. Even in years with annual climate values outside the range of those used to fit the model, few of the daily covariate combinations are likely to fall outside combinations already seen by the model. For example, warmer air temperatures are expected to result in decreased snowpack throughout most of the Northern Hemisphere, shifting many regions from snow-dominated to rain-dominated hydrology [57], but our model already accounts for the predicted range of future snowpack conditions and the influence of different hydrology types on stream temperature. If future air temperatures are warmer and snow melts earlier, spring conditions will likely resemble past summer conditions, and higher elevations and latitudes may mimic historical conditions at lower elevations and latitudes. Therefore, only the most extreme future conditions (e.g., the warmest sites during the warmest time of year) would be outside of our modeled parameter space. The

production of accurate predictions of future air temperatures, stream flows, and snowpack accumulations to inform climate covariates may be a larger source of error than the stream temperature model.

Model limitations and future directions

While we believe that our results are useful for examining patterns in thermal regimes across landscapes and in conservation planning, our stream temperature predictions should be interpreted within the limitations of the modelling approach and prediction accuracy. Prediction error was low on average, however local model residuals should be consulted before using predictions for finer scale applications. Our methods produced predictions representing well-mixed mainstem temperatures of stream reaches that were generally ~1-2 km in length. Accordingly, the model does not reflect finer scale thermal heterogeneity from features such as localized groundwater inputs, backwater areas, deep pools, or localized riparian shading. Such heterogeneity can have important impacts on biota. Similarly, as with other statistical models, the model is not designed to predict temperatures in stagnant or thermally stratified waters such as slow-moving pools, lakes, or reservoirs [5,21].

The model does not account for flow regulation and dam operations; we therefore did not predict stream temperature for reaches likely to be influenced by dams. Because regulated watersheds often produce unnatural flow conditions and thermal regimes [56], statistical models have difficulty accurately predicting below dams (e.g., [24,35,50] without additional dam-specific covariates [5]. Larger dams often release water from below the thermocline in the reservoir, which can lead to large differences in stream temperature (e.g., reductions in the summer and increases in the winter) that can persist many kilometers downstream of the dam [58]. The strength of these effects depends on the size of the dam and how it is managed, discharge volume, water release temperature, and environmental conditions like flow and air temperature [48,58]. These factors make accounting for dam impacts in a spatially expansive model like ours particularly difficult. An analysis comparing empirical measurements of stream temperature to predictions from our existing model (that did not account for dams) would provide insights into dam-specific spatiotemporal impacts on stream temperature and potentially could inform the development of covariates to account for the impact of dams across a regional scale.

Local geology is one of the main factors controlling groundwater influence on stream temperatures [59:62]. For example, [63] found that water temperature in western Oregon streams underlaid by volcanic rock >7 million years old (Western Cascades) was more synchronous with air temperature compared to streams underlaid by volcanic rock <2 million years old (High Cascades),

inferring that groundwater played a larger role in the geologically younger, High Cascades streams. Here, we included the percent of the watershed covered by extrusive volcanic rock (V), but it is unclear how broadly this applies to other regions. The depth of groundwater aquifers can also be important in determining groundwater influence on surface stream temperature [64]. Although we represented potential surface-subsurface interactions with an index of base flow (BFI), it is difficult to empirically assess groundwater inputs and losses at a large spatial scale. However, a recently developed base flow model produced by [65] seems a promising way to improve representation of the interaction of subsurface and surface water on stream temperature. In addition, planform and longitudinal channel morphology influences rates of surface and hyporheic aquifer exchange, and thus stream temperature, in a complex and not well characterized manner [66], that is strongly influenced by the degree of riverscape impairment, particularly floodplain disconnection [67]. Thus, more detailed riverscape context could be incorporated as new covariates or used to define more stream types beyond snow-dominated, rain-dominated, and transitional [68].

Vegetation covariates (i.e., canopy cover and riparian shading) in this and other statistical stream temperature models are temporally constant [5,21, this study], but vegetation cover changes seasonally and spatially [69] and will likely be impacted by climate change. Future improvements should attempt to incorporate vegetation as a temporal covariate. Similarly, the effect of wildfires should be incorporated because wildfires can dramatically decrease riparian vegetation and alter flow paths, impacting stream temperatures, with the strength and direction of the effect varying by season and the severity and location of the wildfire [70,71]. Furthermore, it is likely that the impacts of wildfires on stream temperature will increase as wildfire severity and frequency intensify with climate change [72:74].

Conclusions

Our stream temperature model produced accurate daily predictions for more than 25 years across a large and geographically diverse region and shows promise for application to novel locations and periods. The rich dataset of predicted stream temperature we provide has numerous potential real-world applications for aquatic species and habitat management. Our results can be used to enhance the general understanding of thermal processes in rivers and can help practitioners examine how patterns in thermal regimes vary across the landscape and over time [75]. This approach is simple and flexible enough to be applied in other regions or for different time periods if stream temperature and covariate data are available in those areas and times. The covariate data we used are publicly available

throughout the contiguous United States, which enables easy application of our model in other regions. In addition, new covariates can easily be incorporated into our approach should better spatial or climate data become available. Our model grew from a strong foundation of past research, and we hope that future research will continue to improve its utility and support continued advancement in stream temperature modeling.

Acknowledgements

We thank the NorWeST project for compiling and sharing empirical stream temperature data for the PNW. We thank Valerie Ouellet and David Boughton for constructive feedback during internal review that improved the quality of the manuscript. This research was supported by funds from NOAA Fisheries.

Data availability

Authors will provide code and data upon acceptance of the manuscript.

Authorship CRediT

JES: Conceptualization, Data Curation, Formal Analysis, Methodology, Software, Validation; Writing – Original Draft Preparation; Writing – Review & Editing. AHF: Conceptualization, Data Curation, Software, Visualization, Project Administration, Writing – Original Draft Preparation; Writing – Review & Editing. AMF: Conceptualization; Formal Analysis; Validation; Visualization; Writing – Original Draft Preparation; Writing – Review & Editing. DH: Visualization. CEJ: Conceptualization; Methodology; Project Administration; Resources; Supervision; Writing – Review & Editing.

References

1. Raphael JM. Prediction of temperature in rivers and reservoirs. Journal of the Power Division. 1962;88:157-182. doi: 10.1061/JPWEAM.0000338.

2. Ouellet V, St-Hilaire A, Dugdale SJ, Hannah DM, Krause S, Proulx-Ouellet S. River temperature research and practice: Recent challenges and emerging opportunities for managing thermal habitat conditions in stream ecosystems. Science of the Total Environment. 2020;736:139679. doi: 10.1016/j.scitotenv.2020.139679.

3. Kaushal SS, Likens GE, Jaworski NA, Pace ML, Sides AM, Seekell D, et al. Rising stream and river temperatures in the United States. Frontiers in Ecology and the Environment. 2010;8:461-466. doi: 10.1890/090037.

4. Van Vliet MTH, Ludwig F, Zwolsman JJG, Weedon GP, Kabat P. Global river temperatures and sensitivity to atmospheric warming and changes in river flow. Water Resources Research. 2011;47:W02544. doi: 10.1029/2010wr009198.

5. Isaak DJ, Wenger SJ, Peterson EE, Ver Hoef JM, Nagel DE, Luce CH, et al. The NorWeST summer stream temperature model and scenarios for the western U.S.: a crowd-sourced database and new geospatial tools foster a user community and predict broad climate warming of rivers and streams. Water Resources Research. 2017;WR020969. doi: 10.1002/2017wr020969.

6. Comte L, Buisson L, Daufresne M, Grenouillet G. Climate-induced changes in the distribution of freshwater fish: observed and predicted trends. Freshwater Biology. 2013;58:625-639. doi: 10.1111/fwb.12081.

7. Isaak DJ, Wenger SJ, Young MK. Big biology meets microclimatology: defining thermal niches of ectotherms at landscape scales for conservation planning. Ecological Applications. 2017;27:977-990. doi: 10.1002/eap.1501.

8. Crozier LG, McClure MM, Beechie TJ, Bograd SJ, Boughton DA, Carr M, et al. Climate vulnerability assessment for Pacific salmon and steelhead in the California Current Large Marine Ecosystem. PLOS One. 2019;14: e0217711. doi: 10.1371/journal.pone.0217711.

9. Troia MJ, Kaz AL, Niemeyer JC, Giam X. Species traits and reduced habitat suitability limit efficacy of climate change refugia in streams. Nature Ecology & Evolution. 2019;3:1321-1330. doi: 10.1038/s41559-019-0970-7.

10. Kocik JF, Hayes SA, Carlson SM, Cluer B. A Resist-Accept-Direct (RAD) future for salmon in Maine and California: salmon at the southern edge. Fisheries Management and Ecology. 2022;29(4): 456-474. doi: 10.1111/fme.12575.

11. Isaak DJ, Peterson EE, Ver Hoef JM, Wenger SJ, Falke JA, Torgersen CE, et al. Applications of spatial statistical network models to stream data. Wiley Interdisciplinary Reviews: Water. 2014;1:277-294. doi: 10.1002/wat2.1023.

12. O'Donnell D, Rushworth A, Bowman AW, Scott EM, Hallard M. Flexible regression models over river networks. Applied Statistics. 2014;63:47-63. doi: 10.1111/rssc.12024
13. Caissie D. The thermal regime of rivers: a review. Freshwater Biology. 2006;51:1389-1406. doi: 10.1111/j.1365-2427.2006.01597.x.
14. Dugdale SJ, Hannah DM, Malcolm IA. River temperature modelling: a review of process-based approaches and future directions. Earth-Science Reviews. 2017;175:97-113. doi: 10.1016/j.earscirev.2017.10.009.
15. Pike A, Danner E, Boughton D, Melton F, Nemani R, Rajagopalan B, et al. Forecasting river temperatures in real time using a stochastic dynamics approach. Water Resources Research. 2013;49:5168-5182. doi: 10.1002/wrcr.20389.
16. Benyahya L, Caissie D, St-Hilaire A, Ouarda TBMJ, Bobée B. A review of statistical water temperature models. Canadian Water Resources Journal. 2007;32:179-192. doi: 10.4296/cwrj3203179.
17. Benyahya L., St-Hilaire A, Ouarda TBMJ, Bobée B, Ahmadi-Nedushan, B. Modeling of water temperatures based on stochastic approaches: case study of the Deschutes River. Journal of Environmental Engineering and Science. 2007;6:437-448. doi: 10.1139/s06-067.
18. Hague MJ, Patterson DA. Evaluation of statistical river temperature forecast models for fisheries management. North American Journal of Fisheries Management. 2014;34:132-146. doi: 10.1080/02755947.2013.847879.
19. Peterson DP, Wenger SJ, Rieman BE, Isaak DJ. Linking climate change and fish conservation efforts using spatially explicit decision support tools. Fisheries. 2013;38:112-127. doi: 10.1080/03632415.2013.769157.
20. Peterson EE, Ver Hoef JM. A mixed-model moving-average approach to geostatistical modeling in stream networks. Ecology. 2010;91:644-651. doi: 10.1890/08-1668.1.
21. FitzGerald AM, John SN, Apgar TM, Mantua NJ, Martin BT. Quantifying thermal exposure for migratory riverine species: phenology of Chinook salmon populations predicts thermal stress. Global Change Biology. 2021;27:536-549. doi: 10.1111/gcb.15450.
22. Boughton DA, Harrison LR, John SN, Bond RM, Nicol CL, Legleiter CJ, et al. Capacity of two Sierra Nevada rivers for reintroduction of anadromous salmonids: insights from a high-resolution view. Transactions of the American Fisheries Society. 2022;151:13-41. doi: 10.1002/tafs.10334.
23. Siegel JE, Volk, CJ. Accurate spatiotemporal predictions of daily stream temperature from statistical models accounting for interactions between climate and landscape. PeerJ. 2019;7:e7892. doi: 10.7717/peerj.7892.

24. Piccolroaz S, Calamita E, Majone B, Gallice A, Siviglia A, Toffolon M. Prediction of river water temperature: a comparison between a new family of hybrid models and statistical approaches. Hydrological Processes. 2016;30:3901-3917. doi: 10.1002/hyp.10913.
25. Laanaya F, St-Hilaire A, Gloaguen E. Water temperature modelling: comparison between the generalized additive model, logistic, residuals regression and linear regression models. Hydrological Sciences Journal. 2017;62:1078-1093. doi: 10.1080/02626667.2016.1246799.
26. Abidi O, St-Hilaire A, Ouarda TBMJ, Charron C, Boyer C, Daigle A. Regional thermal analysis approach: A management tool for predicting water temperature metrics relevant for thermal fish habitat. Ecological Informatics. 2022;70:101692. doi: 10.1016/j.ecoinf.2022.101692.
27. McNyset K, Volk C, Jordan C. Developing an effective model for predicting spatially and temporally continuous stream temperatures from remotely sensed land surface temperatures. Water. 2015;7:6827-6846. doi: 10.3390/w7126660.
28. Ouarda TBMJ, Charron C, St-Hilaire A. Regional estimation of river water temperature at ungauged locations. Journal of Hydrology. 2022;17:100133. doi: 10.1016/j.hydroa.2022.100133.
29. Jackson FL, Fryer RJ, Hannah DM, Millar CP, Malcolm IA. A spatio-temporal statistical model of maximum daily river temperatures to inform the management of Scotland's Atlantic salmon rivers under climate change. Science of the Total Environment. 2018;612:1543-1558. doi: 10.1016/j.scitotenv.2017.09.010.
30. Jackson FL, Fryer RJ, Hannah DM, Malcolm IA. Predictions of national-scale river temperatures: A visualization of complex space-time dynamics. Hydrological Processes. 2020;34:2823-2825. doi: 10.1002/hyp.13761.
31. Mohseni O, Stefan HG, Erickson TR. A nonlinear regression model for weekly stream temperatures. Water Resources Research. 1998;34:2685-2692. doi: 10.1029/98WR01877.
32. Lisi, PJ, Schindler DE, Cline TJ, Scheuerell MD, Walsh PB. Watershed geomorphology and snowmelt control stream thermal sensitivity to air temperature. Geophysical Research Letters. 2015;42:3380-3388. doi: 10.1002/2015GL064083.
33. McGill LM, Brooks JR, Steel EA. Spatiotemporal dynamics of water sources in a mountain river basin inferred through delta(2)H and delta(18)O of water. Hydrological Processes. 2021;35:e14063. doi: 10.1002/hyp.14063.
34. Yan H, Sun N, Fullerton AH, Baerwalde M. Greater vulnerability of snowmelt-fed river thermal regimes to a warming climate. Environmental Research Letters. 2021;16:054006. doi: 10.1088/1748-9326/abf393.

35. Siegel JE, Fullerton AH, Jordan CE. Accounting for snowpack and time-varying thermal inertia in statistical models for stream temperature. Journal of Hydrology X. 2022;17:100136. doi: 10.1016/j.hydroa.2022.100136.
36. Asarian JE, Robinson C, Genzoli L. Modeling seasonal effects of river flow on water temperatures in an agriculturally dominated California river. Water Resources Research. 2023;59(3),e2022WR032915. doi: 10.1029/2022WR032915.
37. McKay L, Bondelid T, Dewald T, Rea A, Moore R. NHD Plus Verion 2: User Guide. Application-ready geospatial framework of U.S. surface-water data products associated with the USGS National Hydrography Dataset. United State Geological Survey (USGS). 2012. www.horizon-systems.com/nhdplus/.
38. Lehner B, Liermann CR, Revenga C, Vörösmarty C, Fekete B, Crouzet P, et al. High-resolution mapping of the world's reservoirs and dams for sustainable river-flow management. Frontiers in Ecology and the Environment. 2011;9:494-502. doi: 10.1890/100125.
39. Wood SN. Generalized Additive Models: An Introduction with R, Second Edition. 2017. Chapman and Hall/CRC, New York, NY. 496 pp. ISBN 9781498728331.
40. Wood SN. Mixed GAM Computation Vehicle with Automatic Smoothness Estimation. CRAN. 2018. https://cran.uib.no/web/packages/mgcv/mgcv.pdf.
41. Leach JA, Kelleher C, Kurylyk BL, Moore RD, Neilson BT. A primer on stream temperature processes. WIREs Water. 2023:e1643. doi: 10.1002/wat2.1643.
42. Di Luzio M, Johnson GL, Daly C, Eischeid JK, Arnold JG. Constructing retrospective gridded daily precipitation and temperature datasets for the conterminous United States. Journal of Applied Meteorology and Climatology. 2008;47:475-497. doi: 10.1175/2007JAMC1356.1.
43. Broxton P, Zeng X, Dawson N. Daily 4 km gridded SWE and snow depth from assimilated in-situ and modeled data over the Conterminous US, Version 1. Boulder, Colorado USA. NASA National Snow and Ice Data Center Distributed Active Archive Center. 2019. doi: 10.5067/0GGPB220EX6A.
44. Office of Water Prediction. The National Water Model. National Oceanic and Atmospheric Administration. 2021. https://water.noaa.gov.
45. Hill RA, Weber MH, Leibowitz SG, Olsen AR, Thornbrugh DJ. The stream-catchment (StreamCat) dataset: a dataset of watershed metrics for the conterminous United States. JAWRA. 2016;52:120-128. doi: 10.1111/1752-1688.12372.

46. Letcher BH, Hocking DJ, O'Neil K, Whiteley AR, Nislow KH, O'Donnell MJ. A hierarchical model of daily stream temperature using air-water temperature synchronization, autocorrelation, and time lags. PeerJ. 2016;4:e1727. doi: 10.7717/peerj.1727.
47. Cline TJ, Schindler DE, Walsworth TE, French DW, Lisi PJ. Low snowpack reduces thermal response diversity among streams across a landscape. Limnology and Oceanography Letters. 2020;5:254-263. doi: 10.1002/lol2.10148.
48. Mohseni O, Stefan HG. Stream temperature/air temperature relationship: a physical interpretation. Journal of Hydrology. 1999;218:128-141. doi: 10.1016/S0022-1694(99)00034-7.
49. Holthuijzen MF. A comparison of five statistical methods for predicting stream temperature across stream networks. Utah State University. All Graduate Theses and Dissertations. 2017;6535. https://digitalcommons.usu.edu/etd/6535.
50. Arismendi I, Safeeq M, Dunham JB, Johnson SL. Can air temperature be used to project influences of climate change on stream temperature? Environmental Research Letters. 2014;9:084015. doi: 10.1088/1748-9326/9/8/084015.
51. Jorgensen JC, Nicol C, Fogel C, Beechie TJ. Identifying the potential of anadromous salmonid habitat restoration with life cycle models. PLOS One. 2021; 16: e0256792. doi: 10.1371/journal.pone.0256792.
52. Fogel CB, Nicol CL, Jorgensen JC, Beechie TJ, Timpane-Padgham B, Kiffney P, et al. How riparian and floodplain restoration modify the effects of increasing temperature on adult salmon spawner abundance in the Chehalis River, WA. PLOS One. 2021;17:e0268813. doi: 10.1371/journal.pone.0268813.
53. Null SE, Ligare ST, Viers JH. A method to consider whether dams mitigate climate change effects on stream temperatures. Journal of the American Water Resources Association. 2013;49:1456-1472. doi: 10.1111/jawr.12102.
54. Lusardi RA, Bogan MT, Moyle PB, Dahlgren RA. Environment shapes invertebrate assemblage structure differences between volcanic spring-fed and runoff rivers in northern California. Freshwater Science. 2016;35:1010-1022. doi: 10.1086/687114.
55. Phyllis CC, Sturrock AM, Johnson RC, Weber PK. Endangered winter-run Chinook salmon rely on diverse rearing habitats in a highly altered landscape. Biological Conservation. 2018;217:358-362. doi: 10.1016/j.biocon.2017.10.023.
56. Willis AD, Peek RA, Rypel AL. Classifying California's stream thermal regimes for cold-water conservation. PLOS One. 2021;16. doi: 10.1371/journal.pone.0256286.

57. Wieder WR, Kennedy D, Lehner F, Musselman KN, Rodgers KB, Rosenbloom N, et al. Pervasive alterations to snow-dominated ecosystem functions under climate change. Proceedings of the National Academy of Sciences. 2022;119: e2202393119. doi: 10.1073/pnas.220239311.

765 58. Daniels ME, Danner EM. The drivers of river temperatures below a large dam. Water Resources Research. 2020;56:e2019WR026751. doi: 10.1029/2019WR026751.

59. Kurylyk BL, MacQuarrie KTB, Caissie D, McKenzie JM. Shallow groundwater thermal sensitivity to climate change and land cover disturbances: derivation of analytical expressions and implications for stream temperature modeling. Hydrology and Earth System Sciences. 2015;19(5): 2469-2489. doi:

770 10.5194/hess-19-2469-2015.

60. Johnson ZC, Snyder CD, Hitt NP. Landform features and seasonal precipitation predict shallow groundwater influence on temperature in headwater streams. Water Resources Research. 2017;53: 5788-5812. doi: 10.1002/2017WR020455.

61. Briggs MA, Johnson ZA, Snyder CD, Hitt NP, Kurylyk BL, Lautz L, et al. Inferring watershed hydraulics

775 and cold-water habitat persistence using multi-year air and stream temperature signals. Science of the Total Environment. 2018;636: 1117-1127. doi: 10.1016/j.scitotenv.2018.04.344.

62. Johnson ZC, Johnson BG, Briggs MA, Devine WD, Snyder CD, Hitt NP, et al. Paired air-water annual temperature patterns reveal hydrogeological controls on stream thermal regimes at watershed to continental scales. Journal of Hydrology. 2020;587: 124929. doi: 10.1016/j.jhydrol.2020.124929.

780 63. Tague C, Farrell M, Grant G, Lewis S, Rey S. Hydrogeologic controls on summer stream temperatures in the McKenzie River basin, Oregon. Hydrological Processes. 2007;21: 3288-3300. doi: 10.1002/hyp.6538.

64. Hare DK, Helton AM, Johnson ZC, Lane JW, Briggs MA. Continental-scale analysis of shallow and deep groundwater contributions to streams. Nature Communications. 2021;12: 1450. doi: 10.1038/s41467-021-21651-0.

785 65. Lombard PJ, Dudley RW, Collins MJ, Saunders R, Atkinson E. Model estimated baseflow for streams with endangered Atlantic Salmon in Maine, USA. River Research and Applications. 2021;37: 1254-1264. doi: 10.1002/rra.3835.

66. Tonina D, Buffington JM. Hyporheic exchange in mountain rivers I: mechanics and environmental effects. Geography Compass. 2009;3:1063-1086. doi: 10.1111/j.1749-8198.2009.00226.x.

790 67. Weber N, Bouwes N, Pollock MM, Volk C, Wheaton JM, Wathen G, et al. Alteration of stream temperature by natural and artificial beaver dams. PLOS ONE. 2017;12:e0176313. doi: 10.1371/journal.pone.0176313.

68. Brierley G, Fryirs K. Truths of the riverscape: moving beyond command-and-control to geomorphologically informed nature-based river management. GeoSci Letters. 2022;9:2-26. doi: 10.1186/s40562-022-00223-0.

69. Homer C, Dewitz J, Jin S, Xian G, Costello C, Danielson P, et al. Conterminous United States land cover change patterns 2001–2016 from the 2016 national land cover database. ISPRS Journal of Photogrammetry and Remote Sensing. 2020;162:184-199. doi: 10.1016/j.isprsjprs.2020.02.019.

70. David AT, Asarian JE, Lake FK. 2018. Wildfire smoke cools summer river and stream water temperatures. Water Resources Research 54:7273-7290. doi: 10.1029/2018wr022964.

71. Beyene MT, Leibowitz SG, Snyder M, Ebersole JL, Almquist VW. Variable wildfire impacts on the seasonal water temperatures of western US streams: a retrospective study. PLOS One. 2022;17:e0268452. doi: 10.1371/journal.pone.0268452.

72. Marlon JR, Bartlein PJ, Walsh MK, Harrison SP, Brown KJ, Edwards ME, et al. Wildfire responses to abrupt climate change in North America. Proceedings of the National Academy of Sciences. 2009;106:2519-2524. doi: 10.1073/pnas.0808212106.

73. Abatzoglou JT, Williams AP. Impact of anthropogenic climate change on wildfire across western US forests. Proceedings of the National Academy of Sciences. 2016;113:11770-11775. doi: 10.1073/pnas.1607171113.

74. Halofsky JE, Peterson DL, Harvey BJ. Changing wildfire, changing forests: the effects of climate change on fire regimes and vegetation in the Pacific Northwest, USA. Fire Ecology. 2020;16:1-26. doi: 10.1186/s42408-019-0062-8.

75. Steel EA, Beechie TJ, Torgersen CE, Fullerton AH. Envisioning, quantifying, and managing thermal regimes on river networks. Bioscience. 2017;67:506-522. doi: 10.1093/biosci/bix047.

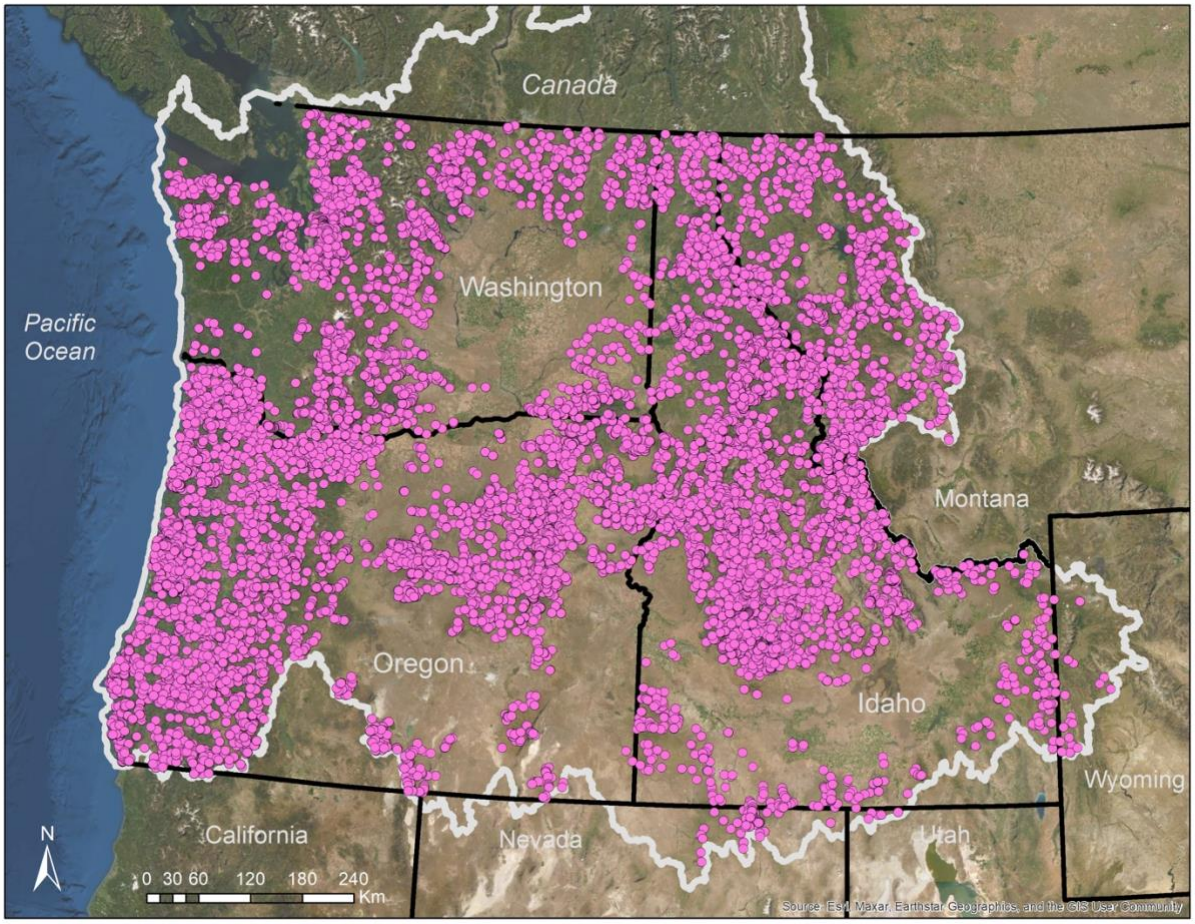

Fig 1: Locations of daily stream temperature data from NorWeST that we used to fit our model, filtered to omit any locations influenced by large dams.

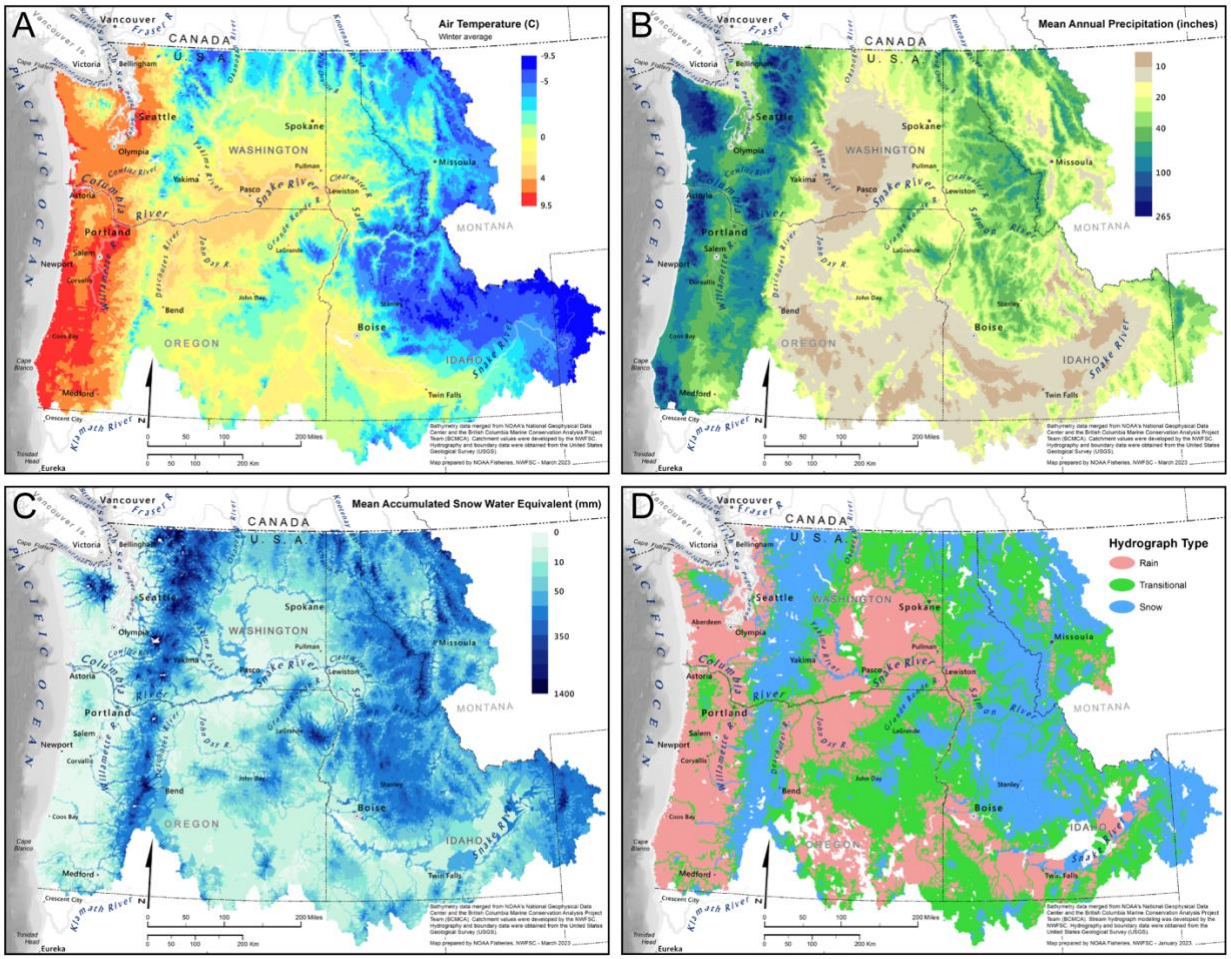

Fig 2: Maps of the PNW illustrating (A) winter average air temperature and (B) mean annual precipitation from the PRISM dataset, (C) mean accumulated snow water equivalent (SWE) in upstream watersheds from the National Snow Water and Ice Dataset, and (D) regions classified in this paper as having rain-dominated, transitional, and snow-dominated hydrology. The mean accumulated snow water equivalent (SWE) was used to classify the hydrograph classes shown in (D). Here, we show the average snowpack accumulation and most common hydrograph classification across the entire dataset. For the analyses annual values were used.

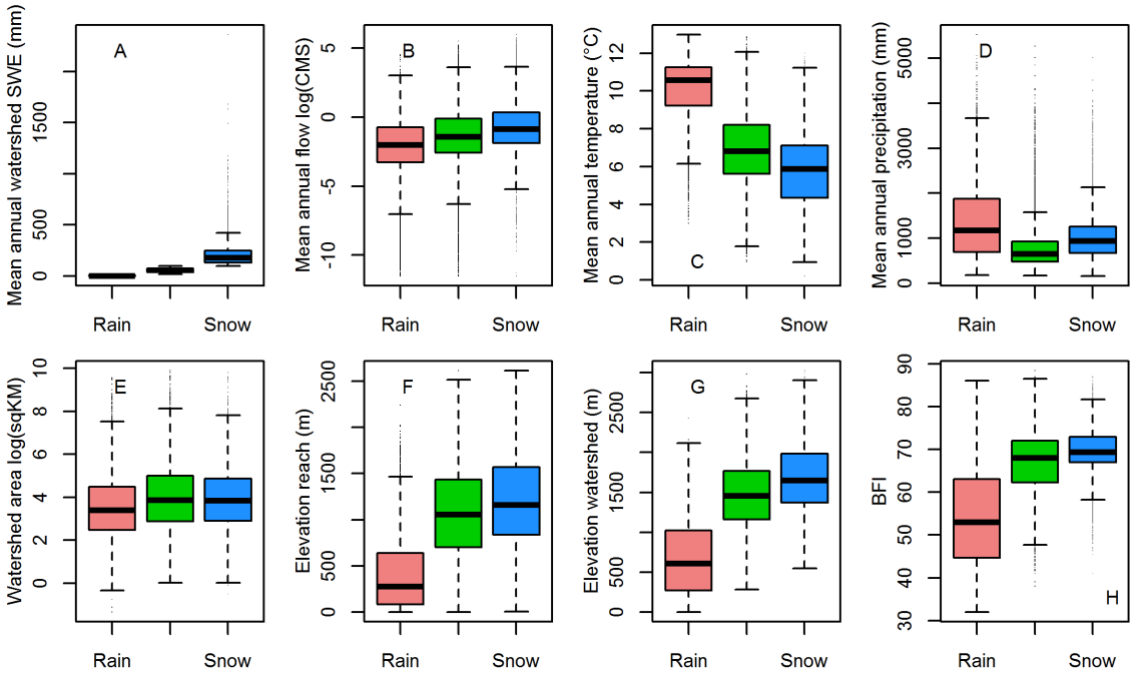

Fig 3: Environmental characteristics of data designated as having “rain”, “transitional”, or “snow” dominated hydrographs. Boxplots show medians, interquartile ranges, and ranges across reach/year combinations. Abbreviations: BFI = baseflow index; CMS = cubic meters per second; SWE = snow water equivalent.

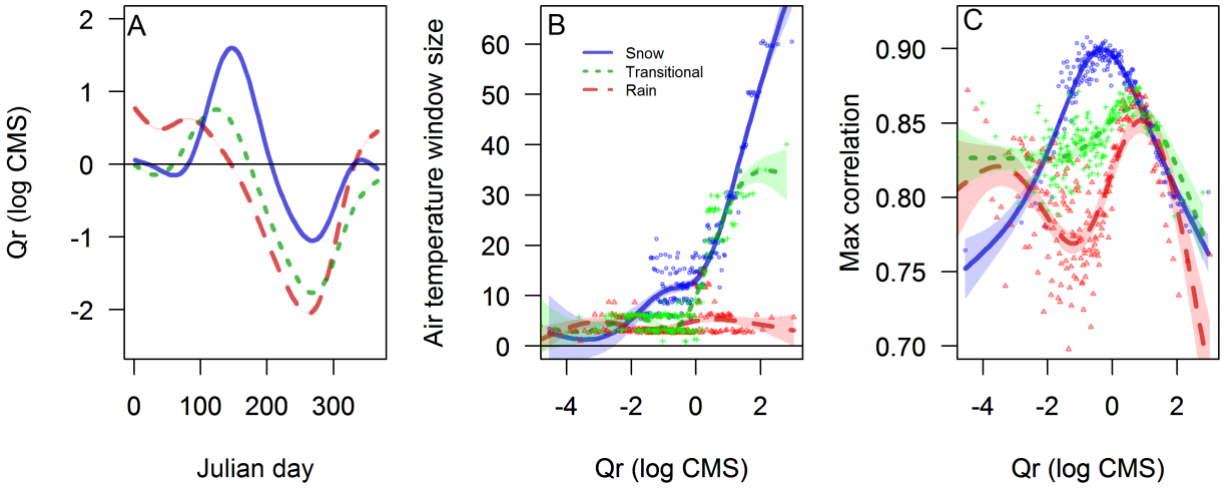

Fig 4: Smoothed patterns for rain, transitional, and snow reaches illustrating (A) area-standardized flow residual (*Qr)* over the year, (B) antecedent air temperature window size with the highest correlation with stream temperature versus average *Qr*, and (C) maximum correlation between stream temperature and antecedent air temperature versus *Qr*.

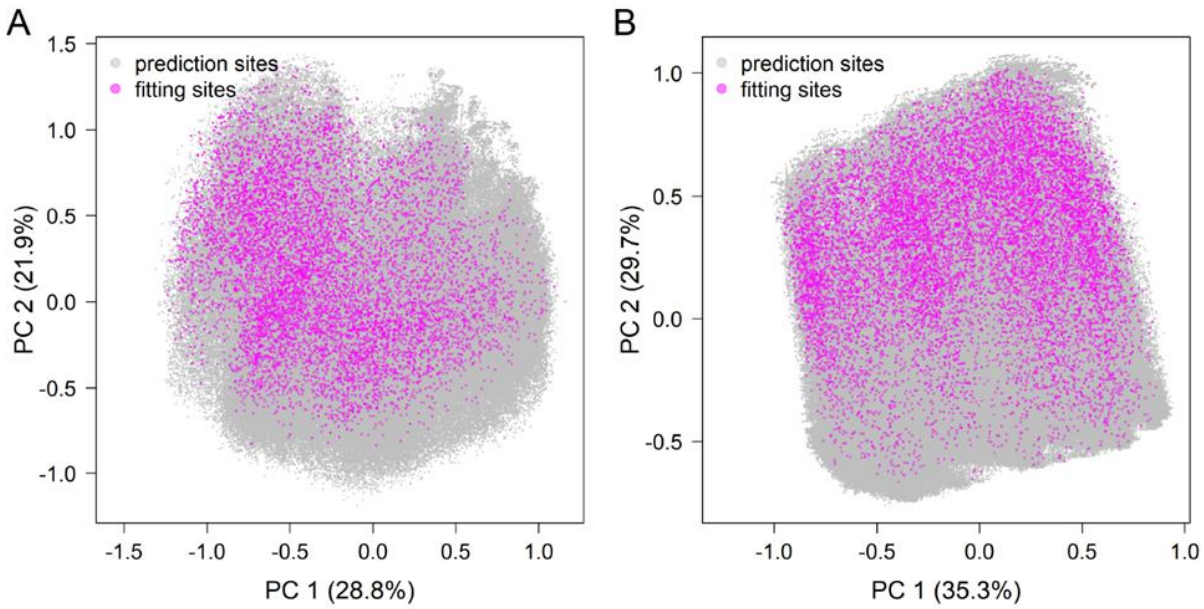

Fig 5: PCA of (A) spatial and (B) temporal covariates used in the stream temperature model, indicating that reaches and days with empirical data that were used when fitting models (magenta) are broadly representative of the parameter space for predicting into locations throughout the full region (gray). The spatial dataset used all data; the temporal dataset used a random 10% of reach-days, aggregated by month.

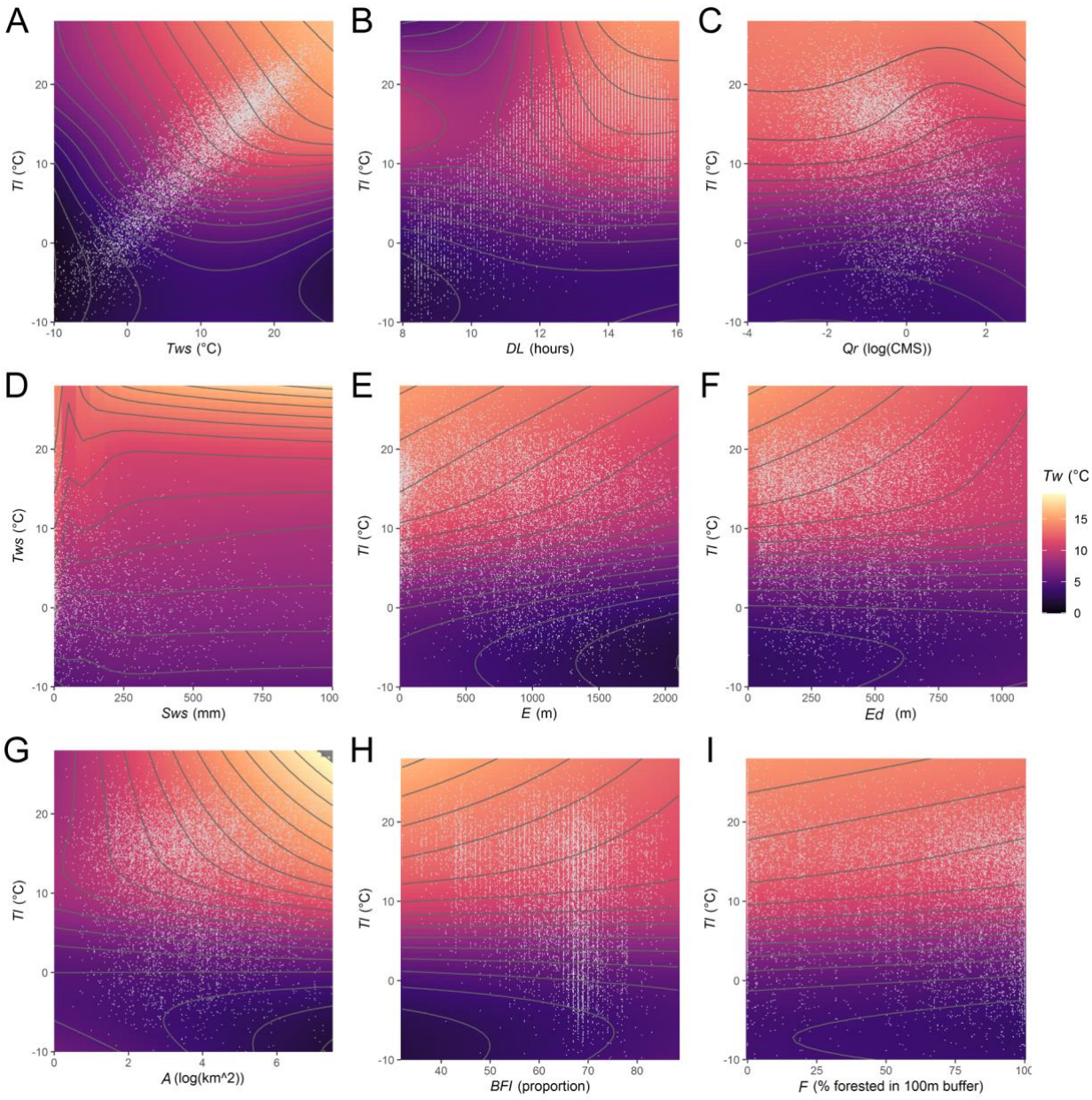

Fig 6: Conditional effect plots for climate and landscape covariates. All interactions we included in the model are shown. Contours represent 1 °C variation in predicted stream temperature. White dots represent empirical data. See Table 1 for covariate definitions.

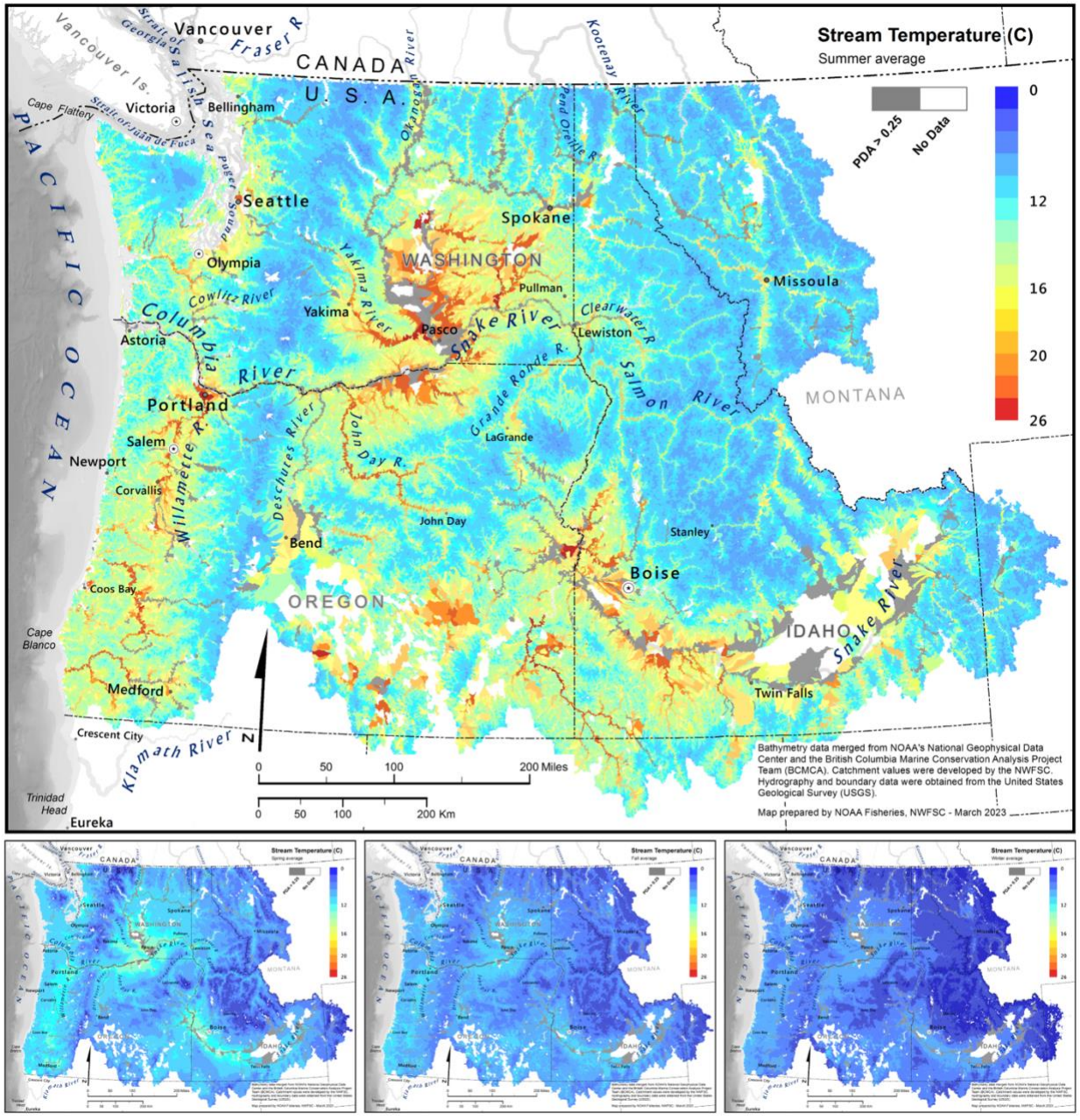

Fig 7. Stream temperature predictions averaged by season (top panel: summer; bottom panels: spring, fall, winter) to illustrate of the spatial extent over which predictions were made and temporal variability. Values were mapped to individual reach-contributing areas to improve visualization, but daily data are linked to each stream reach identifier in the National Hydrography Dataset version 2. Gray indicates reaches where we did not make predictions such as in reservoirs or because reaches were heavily influenced by dams (PDA > 0.25).

Supplementary materials

Table S1: Loadings for the spatial PCA. See Table 1 for covariate definitions.

	PC1	PC2	PC3
C	-0.482	0.010	0.120
P	-0.442	-0.056	0.047
F	-0.436	-0.260	0.235
R	0.425	-0.060	0.191
Lat	-0.301	0.086	0.066
E	0.198	-0.419	0.233
S	-0.173	-0.438	-0.105
BFI	0.126	-0.265	0.376
U	-0.106	0.430	-0.332
A	0.081	0.390	0.385
Ed	-0.078	0.177	0.542
W	-0.036	0.325	0.319
I	-0.032	0.071	0.154
V	0.013	0.034	0.055

Table S2: Loadings for the temporal PCA. See Table 1 for covariate definitions.

	PC1	PC2	PC3
Tws	0.603	0.064	-0.037
Tl	0.596	0.111	-0.055
DL	0.440	0.258	0.283
Sws	-0.239	0.256	0.298
Q	-0.143	0.725	-0.093
Qr	-0.072	0.309	0.684

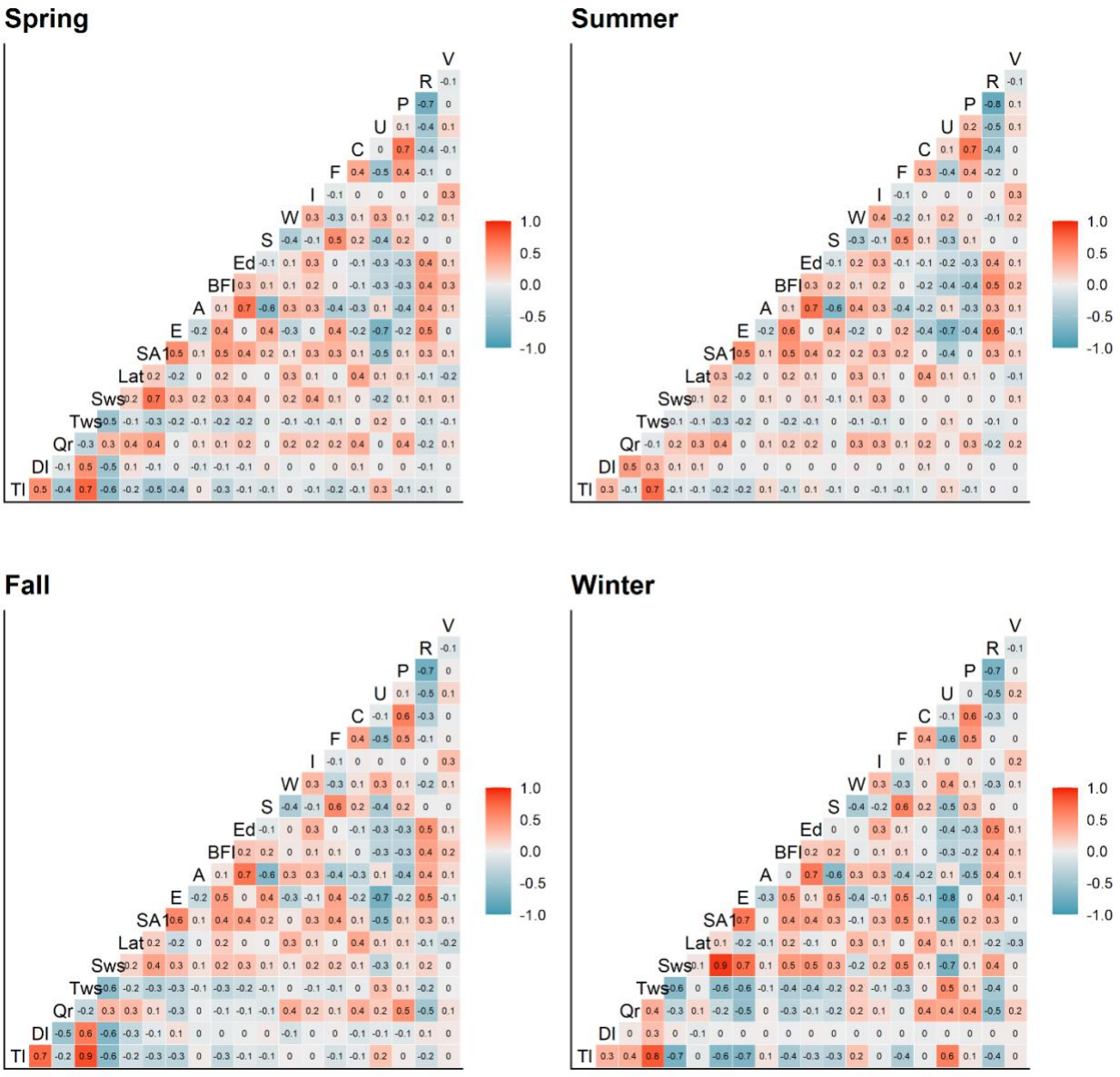

Fig S1: Seasonal correlation plots. Covariate names can be found in Table 1.

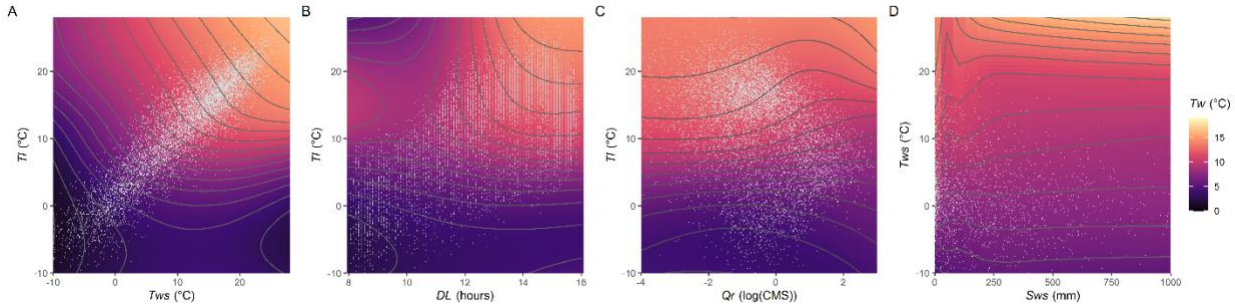

Fig S2: Conditional effect plots for all continuous climate covariates included in the daily stream temperature model. Contours represent 1 degree Celsius variation in predicted stream temperature. White dots represent 10,000 randomly selected empirical data points from dataset. See Table 1 for covariate definitions. All interactions we included in the model are included in Figs S1-S3 (some are shown here and in Fig 6).

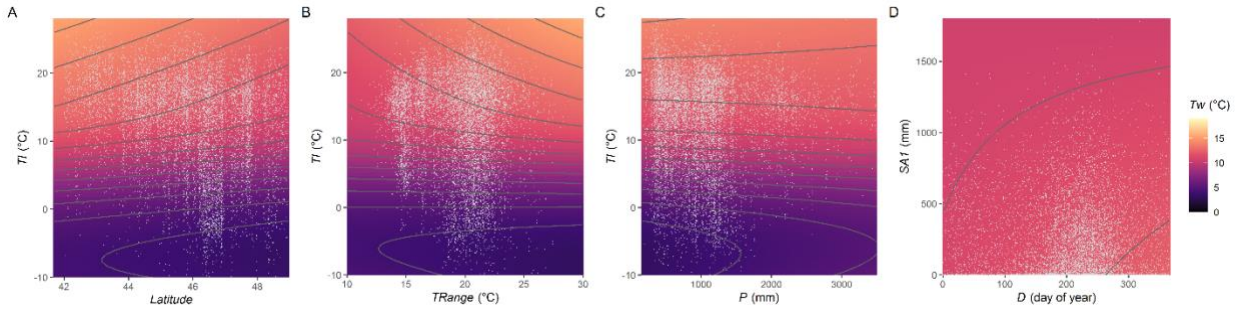

Fig S3: Conditional effect plots for all non-continuous climate covariates included in the daily stream temperature model. Contours represent 1 degree Celsius variation in predicted stream temperature. White dots represent 10,000 randomly selected empirical data points from dataset. See Table 1 for covariate definitions. All interactions we included in the model are included in Figs S1-S3 (some are shown here and in Fig 6).

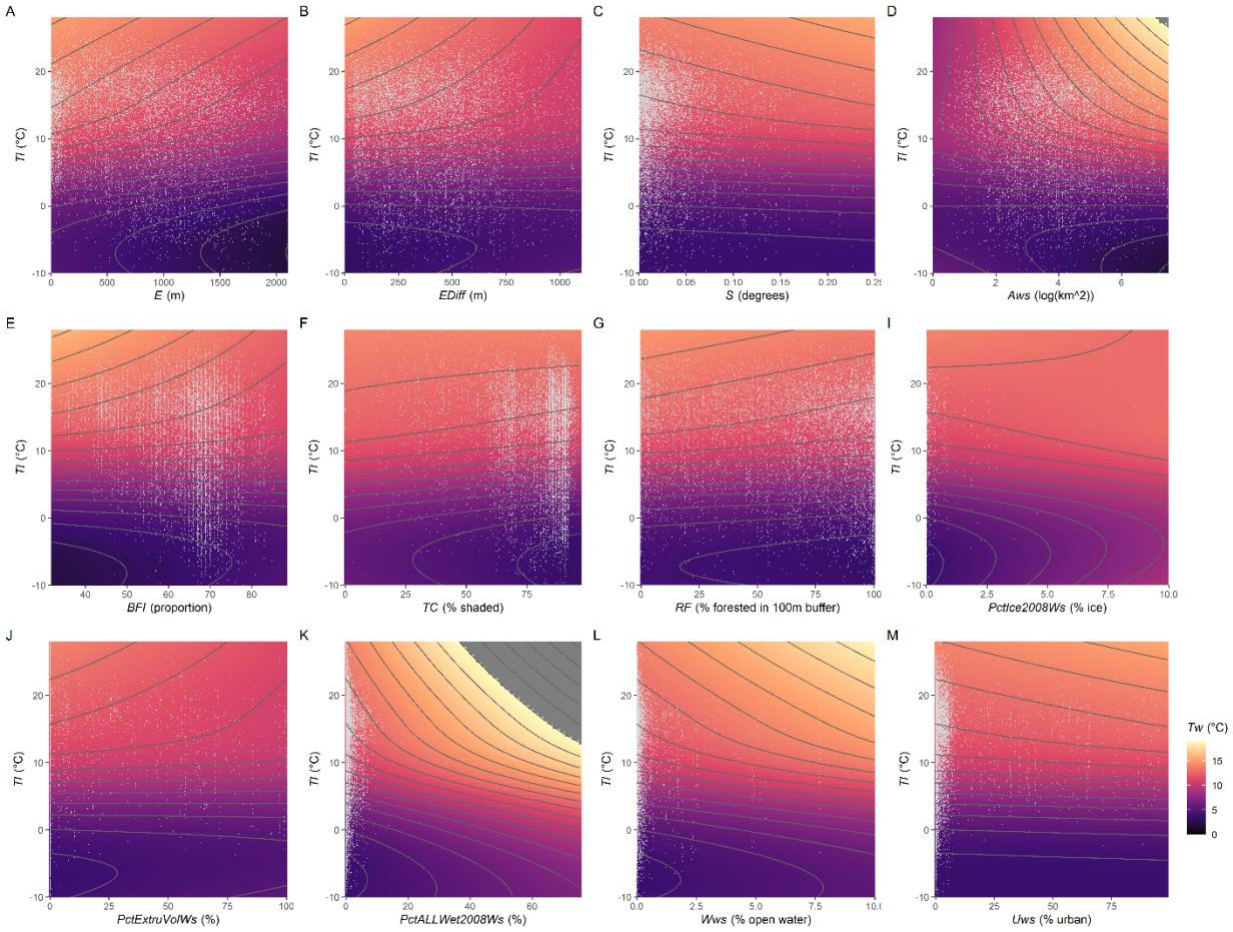

Fig S4: Conditional effect plots for all physical covariates included in the daily stream temperature model. Contours represent 1 degree Celsius variation in predicted stream temperature. White dots represent 10,000 randomly selected empirical data points from dataset. See Table 1 for covariate definitions. All interactions we included in the model are included in Figs S1-S3 (some are shown here and in Fig 6).